Cross sections for the ^{54}Fe(n, n′) ^{54}Fe and ^{54}Fe(n, p′) ^{54}Mn reactions deduced from the detection of de-excitation γ rays

S. F. Hicks[1,2,*], *R. L.* Pecha[2], *T. J.* Howard[2], *A. J.* French[3], *Z. C.* Santonil[2], *J. R.* Vanhoy[4], *A. P. D.* Ramirez[1], *E. E.* Peters[5], *S. H.* Liu[1], *F. M.* Prados-Estevez[1], *T.J.* Ross[1], *B. P.* Crider[1], and *S. W.* Yates[1,5]

[1]Department of Physics and Astronomy, University of Kentucky, Lexington, Kentucky, 40506-0055, USA
[2]Department of Physics, University of Dallas, Irving, Texas, 75062-4736, USA
[3]Department of Chemistry, University of Dallas, Irving, Texas, 75062-4736, USA
[4]Department of Physics, United States Naval Academy, Annapolis, Maryland, 21402-1300, USA
[5]Department of Chemistry, University of Kentucky, Lexington, Kentucky, 40506-0055, USA

Abstract. γ-ray production cross sections have been deduced for reactions with incident neutrons having energies from 1.5 - 4.7 MeV. Similar measurements were made on a natural Ti sample to establish an absolute normalization. The resulting γ-ray production cross sections are compared to TENDL and TALYS calculations, as well as data from previous measurements. The models are found to describe the production cross sections for most γ rays observed from ^{54}Mn and ^{54}Fe rather well.

1 Introduction

Iron is an important component of many structural materials, including energy production complexes, laboratories, devices, and shipping containers that often cross borders. The properties of iron alloys in structural materials—strength, ductility, and stability—depend on defects that develop and grow from neutron induced reactions.

^{54}Fe is only 5.8% abundant in natural Fe, but an examination of neutron total cross sections for incident neutron energies from 1 to 5 MeV reveals that fluctuations from ≈ 1 - 10 b occur for both ^{54}Fe and ^{56}Fe [1]; lower abundance ^{54}Fe can have an out sized contribution to the scattering in regions where it has a cross section maximum and ^{56}Fe has a scattering minimum.

Neutron scattering cross sections obtained by the detection of the scattered neutrons offer the clearest path to the desired neutron scattering cross sections in the fast neutron region [2, 3], but such measurements are typically limited to scattering from only the lowest few excited levels because of the large energy spreads (tens to hundreds of keV) inherent in neutron detection experiments. The detection of de-excitation γ rays (a few keV resolution) following inelastic scattering or proton production for neutrons incident on ^{54}Fe offers a rare opportunity to investigate (n,n′) and (n,p) cross sections, respectively, to higher-lying levels in a consistent way by the examination of γ-ray production rates, as has been reported previously in Refs. [4, 5].

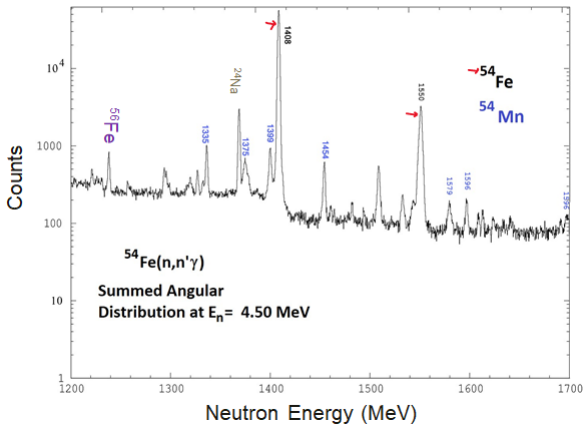

Figure 1. γ-ray spectrum from the summed angular distribution data at E_n = 4.5 MeV. γ-ray energies denoted in blue are from ^{54}Fe(n,p′γ)^{54}Mn and those denoted in black with a red arrow are from ^{54}Fe(n,n′γ)^{54}Fe reactions. Unlabeled peaks are from unplaced γ rays, isotopic impurities or background.

2 Experimental details and data analysis

Measurements were performed at the University of Kentucky Accelerator Laboratory (UKAL) using the neutron production and γ-ray detection facilities developed there over many years. A pulsed beam of protons with a time spread of ≈ 1 ns was accelerated using a model CN Van de Graaff and produced neutrons via the ^{3}H(p,n)^{3}He reaction. The 1 cm × 3 cm (diameter × length) stainless steel ^{3}H cell with a 0.13 mil Mo air-cooled entrance foil, Ta liner and Ta stopper disk was oriented with its length parallel to the beam axis; the gas pressure was ≈ 1 atm.

*e-mail: hicks@udallas.edu

Table 1. Scattering sample masses, geometries and abundances. Uncertainties in masses are estimated to be half the smallest digit and dimensions 0.01 cm. The high-purity metallic ^{54}Fe sample was leased from the U.S. National Isotope Development Program; the sample assay was provided upon lease. The ^{54}Fe sample was pressed and sintered to 85(5)% density. The ^{nat}Ti sample was elemental with isotopic abundances found from NuDat3.0 at NNDC [6].

Sample	Mass (g)	Diameter (cm)	Height (cm)
^{54}Fe	18.045	1.45	1.50
^{Nat}Ti	44.543	2.23	2.55

^{54}Fe Sample	Assay	^{nat}Ti Sample	Assay
^{54}Fe	97.60(2)%	^{46}Ti	8.25(3)%
^{56}Fe	2.35(2)%	^{47}Ti	7.44(2)%
^{57}Fe	0.04(1)%	^{48}Ti	73.72(3)%
^{58}Fe	0.01(5)%	^{49}Ti	5.41(2)%
		^{50}Ti	5.18(2)%

Samples of ^{54}Fe and ^{nat}Ti were suspended 6.5(1) cm from the center of the gas cell; sample masses, geometries, and isotopic abundances are given in Table 1.

The emitted γ rays were detected with a $\approx$ 50% HPGe detector located 1.15(1) m from the center of the gas cell; this detector was surrounded by an annular BGO detector for active Compton suppression. Both detectors were shielded by boron-loaded polyethylene, copper and a tungsten shadow bar. The γ-ray detector efficiency and energy calibration were completed using a ^{226}Ra radioactive source. Time of flight (TOF) techniques were used to veto neutron events in the main detector.

γ-ray excitation functions and angular distributions following the ^{54}Fe(n,n$'\gamma$)^{54}Fe and ^{54}Fe(n,p$'\gamma$)^{54}Mn reactions were measured for incident neutron energies from 1.5 to 4.7 MeV in 200 keV steps and at E$_n$ = 4.5 MeV, respectively. The excitation functions were measured with the HPGe detector fixed at 125° where $P_2 = 0$ in the Legendre polynomial expansion $\frac{d\sigma}{d\Omega} = A_0[1 + a_2P_2(cos\theta) + a_4P_4(cos\theta)]$; P_l is the Legendre polynomial of order l = 0, 2, 4 and a_l is its coefficient. Provided $a_4 \approx 0$, then the γ-ray production cross section is simply $\sigma = 4\pi A_0$.

Similar measurements were made on natural Ti for absolute normalization. The uncertainty of the neutron energies impinging on the samples averaged $\approx$ 50 keV for the ^{54}Fe and $\approx$ 70 keV for the ^{nat}Ti samples; those uncertainties include proton straggling in the gas cell entrance foil, proton energy loss in the ^{3}H gas cell, and sample geometry. A spectrum is shown in Fig. 1.

γ-ray production cross sections were normalized relatively using a long counter [7]; corrections were made for variations in the detector efficiency and ^{3}H(p, n)^{3}He neutron production cross sections [8] at the position of the long counter (85 deg) as a function of E$_n$ [9]. Uncertainties on all production cross sections include those from the yields of the peaks of interest in the main and monitor spectra, an estimated 4% uncertainty from finite sample corrections (neutron multiple scattering and γ-ray attenuation) [10], a 3% relative uncertainty from the γ-ray detector efficiency, and uncertainty in finding the absolute normalization factor discussed below.

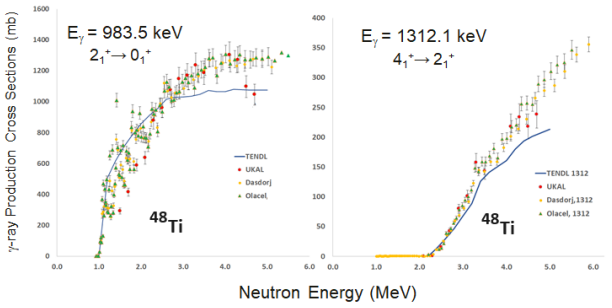

Figure 2. Comparison of UKAL γ-ray production cross sections for the first two excited states of ^{48}Ti at 983.5 and 1312.1 keV with previously published data [12, 13] and TENDL calculations by Koning et al. [14]. An absolute normalization factor for UKAL data was deduced from Ref.[12] by comparing the 983.5 keV γ-ray production cross sections between 2.1 and 4.3 MeV.

To obtain absolute γ-ray production cross sections, the 983.5 keV γ ray from the decay of the first excited state of ^{48}Ti, a reference standard [11], was used, and a normalization factor of $1.13(1)\times10^{-2}$ was found by comparing relative γ-ray production cross sections to those of Dashdorj et al. [12]. Only UKAL production cross sections for the 983.5 keV γ ray between E_n = 2.1 and 4.3 MeV were used in this comparison, since the assumption that $a_4 \approx 0$ was previously found to be valid about $\approx$ 1 MeV above threshold [10] for the strong *E2* transition from the first excited state to the ground state.

The UKAL normalized values were then compared to previous measurements [12, 13] and TENDL cross sections [14], as shown in Fig. 2. While the experimental cross sections do not agree well with the TENDL calculations, they do agree well with each other above 2.1 MeV for the 983-keV γ ray and at all energies for the 1312.1 keV γ ray in ^{48}Ti, with the exception of the two highest neutron energies, which are still being reviewed.

Once an absolute normalization factor was obtained from the ^{48}Ti 983 keV γ ray, the same constant factor, corrected for the difference in the number of target nuclei, was applied to the relative production cross sections of γ rays observed for ^{54}Fe and ^{54}Mn to obtain absolute cross sections.

3 Results and Conclusions

Absolute production cross sections for the strongest γ rays observed from the 4_1^+, 5_1^+, and 3_2^+ levels in ^{54}Mn, along with TENDL calculations [14] and TALYS [15, 16] calculations with default parameters are shown in Fig. 3. The 156.3 keV γ ray is from the lowest excited level observed in the UKAL measurements, as the 54.9 keV 2_1^+ first excited state is below our detection threshold. TENDL calculations [14] do not describe well the γ-ray production from this 4_1^+ state, nor do calculations using TALYS default parameters; however, TENDL model calculations do

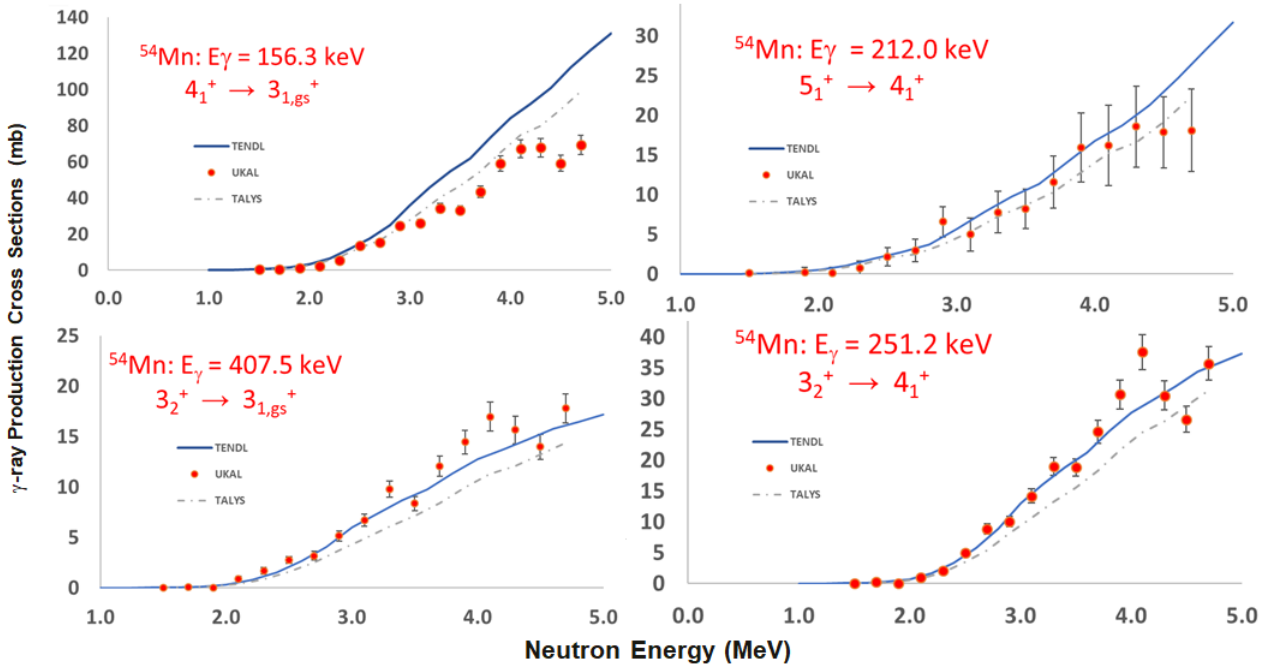

Figure 3. Preliminary production cross sections observed in ^{54}Mn for γ rays from the three lowest observed excited levels (red circles), along with TENDL calculations (blue line) by Koning et al. [14], and calculations performed using TALYS [15, 16] default parameters (gray dotted line).

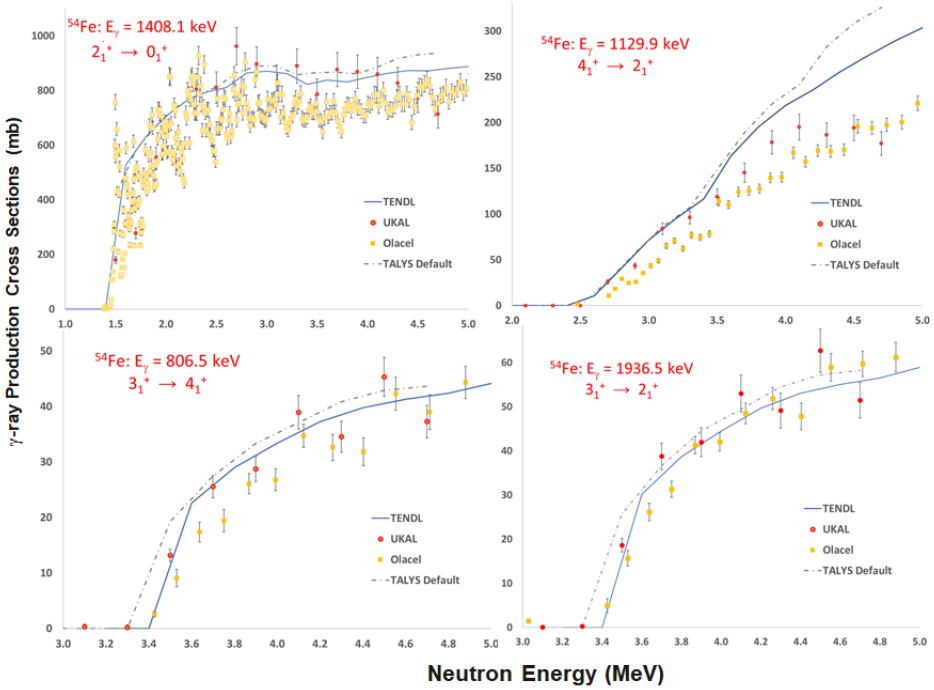

Figure 4. Preliminary ^{54}Fe γ-ray production cross sections for the 1408.2 keV ($2_1^+ \rightarrow 0_1^+$), 1129.9 keV ($4_1^+ \rightarrow 2_1^+$), 806.5 ($3_1^+ \rightarrow 4_1^+$), and 1936.5 keV ($3_1^+ \rightarrow 2_1^+$) decays (red circles), along with TENDL calculations (blue) by Koning et al. [14], TALYS [15, 16] calculations with default parameters (dotted gray), and the results from Olacel et al. (yellow squares) [4].

well describe the production cross sections of the other γ rays shown, as well as most observed production cross sections for γ rays from levels below about 1.6 MeV excitation energy in ^{54}Mn.

^{54}Fe production cross sections are shown in Fig. 4 for γ rays from the 2_1^+, 4_1^+, and 3_1^+ excited states. For the 1408.2 keV γ ray ($2_1^+ \rightarrow 0_1^+$), the UKAL data agree well with TENDL and TALYS calculations, except at E_n

< 2 MeV, or until ≈ 1 MeV above threshold [10], and at the two highest energy points that are still under review. For the 1129.9 keV γ ray ($4_1^+ \rightarrow 2_1^+$), both TENDL and TALYS calculations agree with UKAL data until about 3.5 MeV, but are significantly higher than data from Ref. [4]. Interestingly, for the 806.5 and 1936.5 keV γ rays from the decay of the 3_1^+ level, the first unnatural parity excitation in ^{54}Fe, the TALYS and TENDL calculations are in good agreement with the UKAL data; this agreement suggests that the compound nuclear process of the n + ^{54}Fe interaction is well described. In all cases, the preliminary UKAL γ-ray production cross sections are significantly larger than the data of Ref. [4].

The UKAL data set is very large and is still being analyzed. Additional measurements are in progress that will help us understand the a_2 and a_4 coefficients for the 983.5 keV γ ray in ^{48}Ti and, hopefully, help us explain the differences observed between our measurements and those of Refs. [12, 13] below ≈ 2 MeV. Once all analyses are completed, the deduced production cross sections for γ rays observed from the decay of levels in ^{48}Ti, ^{54}Mn, and ^{54}Fe will be submitted to EXFOR. Another goal is to deduce level cross sections for neutrons reacting with ^{54}Fe.

3.1 ACKNOWLEDGEMENTS

This work was supported by the U.S. Department of Energy NNSA-SSAP award NA-0002931 and Nuclear Energy Universities Program award NU-12-KY-UK-0201-05, the U.S. National Science Foundation under grant PHY-1305801, and the U.S. National Isotope Development Program. The authors would like to thank accelerator engineer Harvey G. Baber for his continued commitment to the operation of the UKAL accelator, and deceased Emeritus Professor Marcus T. McEllistrem, who shared his neutron scattering wisdom very generously early in this project.

References

[1] W, Geel, Private Communication to EXFOR (1995) (EXFOR 22316002 and 22316003)

[2] J. Vanhoy, S. Liu, S. Hicks, B. Combs, B. Crider, A. French, E. Garza, T. Harrison, S. Henderson, T. Howard et al., Nuclear Physics A **972**, 107 (2018)

[3] I.A. Korzh, V.A. Mishchenko, N.M. Pravdivyi, Soviet Atomic Energy **62**, 487 (1987)

[4] A. Olacel, C. Borcea, M. Boromiza, P. Dessagne, G. Henning, M. Kerveno, L. Leal, A. Negret, M. Nyman, A.J.M. Plompen, Eur. Phys. J. A **54**, 183 (2018)

[5] Hicks, S. F., Vanhoy, J. R., French, A. J., Henderson, S. L., Howard, T. J., Pecha, R. L., Santonil, Z. C., Crider, B. P., Liu, S., McEllistrem, M. T. et al., EPJ Web of Conferences **93**, 02002 (2015)

[6] National Nuclear Data Center, information extracted from the NuDat database, https://www.nndc.bnl.gov/nudat/, note = Accessed: 2022-02-05

[7] A.O. Hanson, J.L. McKibben, Phys. Rev. **72**, 673 (1947)

[8] M.Drosg, Tech. Rep. IAEA-NDS-87 Rev. 8, IAEA (2003)

[9] J. Marion, F. Young, *Nuclear Reaction Analysis: Graphs and Tables* (North Holland Publishing, Amsterdam, 1968)

[10] Vanhoy, J.R., Ramirez, A.P., Alcorn-Dominguez, D.K., Hicks, S.F., Peters, E.E., McEllistrem, M.T., Mukhopadhyay, S., Yates, S.W., EPJ Web Conf. **146**, 11051 (2017)

[11] A. Carlson, V. Pronyaev, R. Capote, G. Hale, Z.P. Chen, I. Duran, F.J. Hambsch, S. Kunieda, W. Mannhart, B. Marcinkevicius et al., Nuclear Data Sheets **148**, 143 (2018), special Issue on Nuclear Reaction Data

[12] D. Dashdorj, T. Kawano, P.E. Garrett, J.A. Becker, U. Agvaanluvsan, L.A. Bernstein, M.B. Chadwick, M. Devlin, N. Fotiades, G.E. Mitchell et al., Phys. Rev. C **75**, 054612 (2007)

[13] Olacel, Adina, Belloni, Francesca, Borcea, Catalin, Boromiza, Marian, Dessagne, Philippe, Henning, Gregoire, Kerveno, Maëlle, Negret, Alexandru, Nyman, Markus, Pirovano, Elisa et al., EPJ Web Conf. **146**, 11014 (2017)

[14] A. Koning, D. Rochman, J.C. Sublet, N. Dzysiuk, M. Fleming, S. van der Marck, Nuclear Data Sheets **155**, 1 (2019), special Issue on Nuclear Reaction Data

[15] A. Koning, S. Hilaire, M. Duijvestijn, International Conference on Nuclear Data for Science and Technology, p. 211 (2007)

[16] A. Koning, J. Delaroche, Nuclear Physics A **713**, 231 (2003)